Ultra-Hot-Jupiters in TESS

SuPerPiG
Short Period Planet Group

Elisabeth R. Adams (Planetary Science Institute, adams@psi.edu)
Brian Jackson (Boise State University)

Abstract

Ultra-short-period planets, with periods of less than two days, are skirting right on the edge of destruction. For ultra-hot Jupiters (UHJs), the strongest challenge comes from tides: the closer these massive planets get to their stars, the faster the rate of orbital decay, and the eventual fate of some is to spiral into their stars. Tentative evidence for tidal disruption comes from the distribution of short-period orbits and the metallicities of stars hosting what may be the remnants of tidally disrupted gas giants. However, more direct evidence comes from long-baseline observations of short-period planets that may be undergoing orbital decay. Such is thought to be the fate of WASP-12 b (P=1.09 d), whose orbital period seems to be decreasing (Patra et al., 2017). Not surprisingly, planets that may be inspiralling are intrinsically rare, and there are also not many ultra-hot Jupiters known around bright stars that are easy to monitor from the ground over the decade+ that is required to determine the rate of orbital decay. TESS has already provided dozens of candidates ultra-hot Jupiters, many bright, that are good candidates for observing tidal effects. Unfortunately, ultra-hot Jupiters are accompanied by a high rate of false positives. We demonstrate a heuristic method based solely on TESS photometry that can significantly improve planetary recovery for these massive, tidally-challenged planets, and demonstrate using WASP-18 b, (TIC 100100827, P = 0.94 d), showing how modeling the out-of-transit phase curve variability can be used to efficiently separate eclipsing binaries from ultra-hot Jupiters.

We have fit 110 candidate TOIs with P<2 days for phase variability. Our goal is to develop a heuristic test based on the values for $\mathbf{A_{refl}}$, $\mathbf{A_{beam}}$ and $\mathbf{A_{ellip}}$ that can triage ultra-hot Jupiter candidates into three groups:
A: Promising candidates
B: Likely false positives
C: Everything else

Good candidate traits:
- q_{beam} x 10^3 and q_{ellip} x 10^3 within order of magnitude of 1 (i.e., mass ratio is 10^{-3}, similar to Jupiter and the Sun)
- $\mathbf{A_{refl}}$ positive, less than expected max
- $\mathbf{A_{beam}}$ and $\mathbf{A_{ellip}}$ positive

A

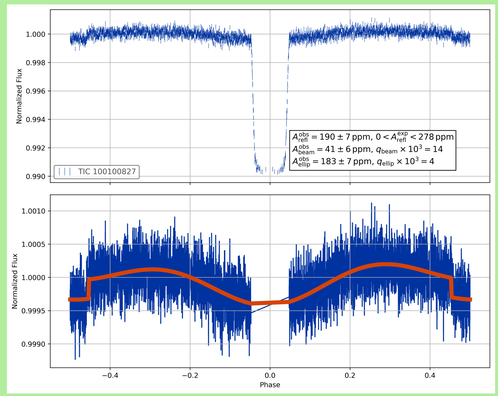

Figure 3. TIC 100100827, good candidate for followup. $\mathbf{A_{refl}}$ is within expected range, and both mass ratios are consistent with planetary. This is WASP-18 b (R_p=13 R_E, P=0.94 d).

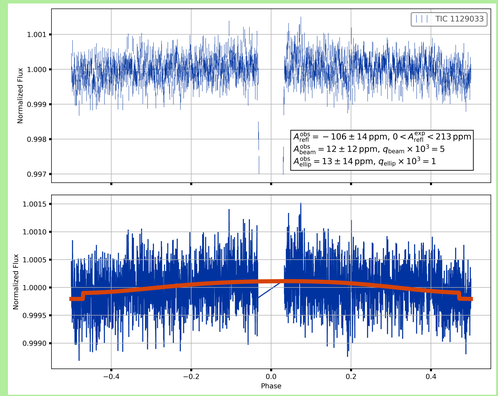

Figure 3. TIC 1129033, good candidate for followup. $\mathbf{A_{refl}}$ is negative, but mass ratios are both consistent with planetary. This is WASP-77 A b (R_p=13.6 R_E, P=1.36 d).

Bottom: phase variability from all components, with central transit remove. Model is plotted in red.

Components of phase variability

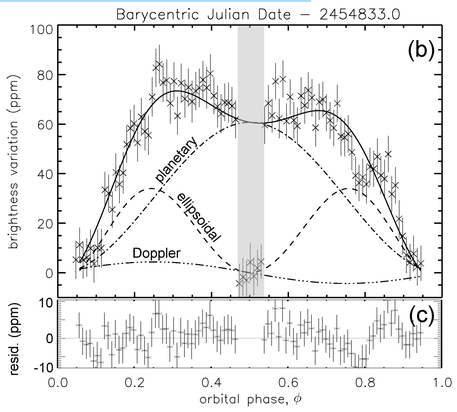

Fig 1. Relative contribution of three components of phase variability, adapted from Fig 5b of Jackson et al. 2012., for HAT-P-7 b; "planetary" refers to the reflection component, "Doppler" to the beaming.

Since planets are not self-luminous, their phase curves result from reflected/re-emitted instellation, with amplitude $\mathbf{A_{refl}}$ related to the ratio of the planet's total luminosity L_p to the host star's $L_\star$, where i is the orbital inclination, p the planet-to-star radius ratio, and $\rho_\star$ the stellar density. (We've assumed the planet is a single temperature blackbody in radiative equilibrium with the host star.)

$$A_{\rm refl} = \frac{1}{2}\frac{L_{\rm p}\sin i/2}{L_\star/2} \approx \frac{1}{4}\left(\frac{R_{\rm p}}{a}\right)^2 \sin i \approx (1.6\times10^{-2})\ p^2 \left(\frac{P}{\rm day}\right)^{-4/3}\left(\frac{\rho_\star}{\rho_\odot}\right)^{-2/3}\sin i \qquad \textbf{Eqn 1.}$$

As discussed in Loeb and Gaudi (2003), the reflex motion of a planet-hosting star results in a small (few ppm) brightening as the star approaches the observer. This is the Doppler, or beaming, component, and its amplitude is $\mathbf{A_{beam}}$, where α_{beam} is a coefficient of order unity that accounts for the finite bandpass of the instrument.

$$A_{\rm refl} = \frac{1}{2}\frac{L_{\rm p}\sin i/2}{L_\star/2} \approx \frac{1}{4}\left(\frac{R_{\rm p}}{a}\right)^2 \sin i \approx (1.6\times10^{-2})\ p^2 \left(\frac{P}{\rm day}\right)^{-4/3}\left(\frac{\rho_\star}{\rho_\odot}\right)^{-2/3}\sin i \qquad \textbf{Eqn 2.}$$

We also include in our model the ellipsoidal variations caused by tidal distortions, which cause the star to become slightly ellipsoidal, with an amplitude $\mathbf{A_{ellip}}$ (from Shporer 2017) given by:

$$A_{\rm ellip} \approx 13\alpha_{\rm ellip}\sin i \times \left(\frac{R_\star}{R_\odot}\right)^3\left(\frac{M_\star}{\rm M_\odot}\right)^{-2}\left(\frac{P}{\rm day}\right)^{-2}\left(\frac{M_{\rm p}\sin i}{\rm M_{Jup}}\right)\ \text{ppm} \qquad \textbf{Eqn 3.}$$

α_{ellip} is a coefficient that accounts for the stellar limb darkening and gravity darkening, where g is the gravity darkening coefficient and u the linear stellar limb darkening coefficients from Claret and Bloemen (2011).

$$\alpha_{\rm ellip} = 0.15\frac{(15+u)(1+g)}{3-u}$$

B

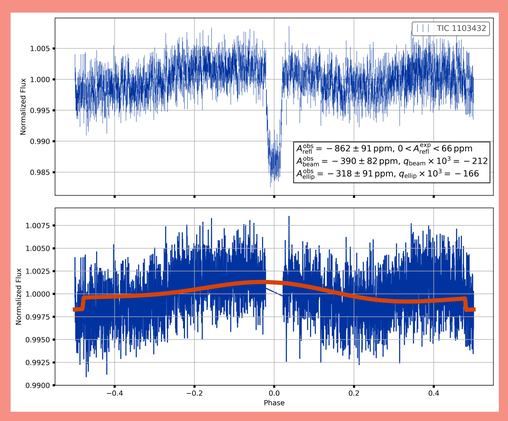

Figure 2. TIC 1103432, high likelihood of false positive. $\mathbf{A_{refl}}$ is strongly negative, and one mass ratio, q_{beam}, is high (a false positive signature), though the other mass ratio, q_{ellip}, is consistent with planetary. Note that mass ratios are not very precise and order of magnitude agreement is sought.

C

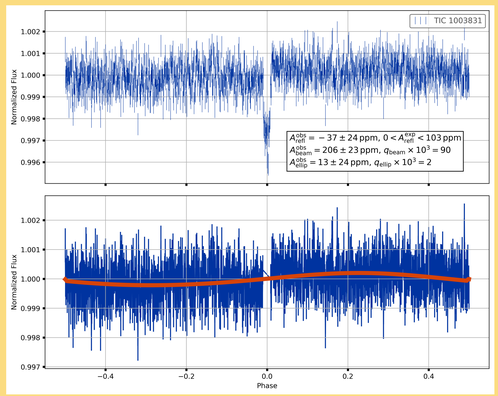

Figure 1. TIC 1003831, ambiguous planet candidate. $\mathbf{A_{refl}}$ is within 1-σ of zero. One mass ratio, q_{beam}, is high (a false positive signature), while the other mass ratio, q_{ellip}, is consistent with planetary. (Note that mass ratios are not very precise and only order of magnitude agreement is sought.)

How these plots were made

1. All TOIs with P < 2 days and values for P, $R_\star$, $M_\star$, and $R_p/R_\star$ as of June 21, 2019 (110 objects) on the TESS ExoFOP (https://exofop.ipac.caltech.edu/tess/).
2. We used lightkurve (http://ascl.net/1812.013) to obtain the TESS target pixel files for each sector each target was observed.
3. For each target pixel file, we used the mission pipeline's optimal aperture mask to create the light curve (https://docs.lightkurve.org/api/lightkurve.targetpixelfile.TessTargetPixelFile.html#lightkurve.targetpixelfile.TessTargetPixelFile.pipeline_mask).
4. Detrended light curve using 2nd-order Savitzky-Golay (i.e., polynomial fit to each point) filter with window size equal to 4 orbital periods for each target.
5. Dropped outliers (20 sigma).
6. Folded all sectors' light curves onto the orbital period and bin 10 points at a time, using the bin median as the datum; per-point uncertainties initially estimated as median absolute deviation, with subsequent χ^2) re-scaling after model fit.
7. Using binned data, fit Mandel-Agol transit model without limb-darkening using Levenburg-Marquardt to confirm the reported timing. (We did not check for transit-timing variations.)
8. Fit sinusoidal model for the reflection, beaming, and ellipsoidal components, rescaling parameter uncertainties by square root of resulting χ^2.. (Fig 5b, right, from Jackson et al. 2012, shows the different components)
9. Estimated the expected reflected component using the Eqn 1. We did NOT use the other scalings (Eqns. 2 and 3) to the estimate beaming and ellipsoidal signals, but we DID use them to convert the observed signals into a mass ratio, assuming the stellar parameters supplied by the table from the TESS ExoFOP.

References

A. Claret and S. Bloemen. Gravity and limb-darkening coefficients for the Kepler, CoRoT, Spitzer, uvby, UBVRIJHK, and Sloan photometric systems. A&A, 529:A75, May 2011. doi: 10.1051/ 0004-6361/201116451.

A. Loeb and B. S. Gaudi. Periodic Flux Variability of Stars due to the Reflex Doppler Effect Induced by Planetary Companions. ApJ, 588:L117–L120, May 2003. doi: 10.1086/375551.

B. Jackson, N. K. Lewis, J. W. Barnes, L. Drake Deming, A. P. Showman, and J. J. Fortney. The EVIL-MC Model for Ellipsoidal Variations of Planet-hosting Stars and Applications to the HAT- P-7 System. ApJ, 751:112, June 2012. doi: 10.1088/0004-637X/751/2/112.

B. Jackson, E. R. Adams, W. Sandidge, S. Kreyche, and J. Briggs. Variability in the Atmosphere of the Hot Jupiter Kepler-76b. AJ, 157, 6.

A. Shporer. The Astrophysics of Visible-light Orbital Phase Curves in the Space Age. PASP, 129 (7):072001, July 2017. doi: 10.1088/1538-3873/aa7112.

A. Shporer, I. Wong, C. X. Huang, M. R. Line, K. G. Stassun, T. Fetherolf, S. Kane, G. R. Ricker, D. W. Latham, S. Seager, J. N. Winn, J. M. Jenkins, A. Glidden, Z. Berta-Thompson, E. B. Ting, J. Li, and K. Haworth. TESS full orbital phase curve of the WASP-18b system. arXiv e-prints, November 2018.